Cause Investigation of Flooding & Sinking Accident of Ro-Ro Ferry Ship using Marine Accident Integrated Analysis System

Sang-Gab Lee, Jae-Seok Lee, Ji-Hoon Park and Tae-Young Jung

Korea Maritime & Ocean University, Marine Safety Technology, Busan, Korea

1 Abstract

Ro-Ro ferry ship was capsized and was sunk down to the bottom in the sea water due to the rapid turning for the several reasons, such as lack of stability and poor lashing, etc. Objective of this study is to figure out the air pocket existence in the flooding & sinking accident using Marin Accident Integrated Analysis System (MAIAS; highly advanced M&S system of Fluid-Structure Interaction analysis technology). Several things were carried for this investigation of air pocket existence, such as accurate ship posture track according to accident duration using several accident photos and movies, precise ship and cargo moving track and sea water inflow amount according to accident duration using floating simulation and hydrostatic characteristics program, accurate understanding of exterior openings and interior paths of sea water inflow, simulation of sea water inflow using flooding & sinking simulation and calculation of exterior openings & interior inflow paths. There was relatively good prediction of air pocket existence.

***Keyword Words**: Ro-Ro Ferry Ship; Flooding & Sinking Accident; Marine Accident Integrated Analysis System (MAIAS); Highly Advanced Modeling & Simulation (M&S) System; Fluid-Structure Interaction (FSI) Analysis Technique; Full-Scale Ship Floating, Flooding & Sinking Simulation; Hydrostatic Characteristics Program.*

2 Introduction

The Ro-Ro ferry ship was capsized 180° about two and half hours later after rapid turning accident with just bow bottom exposed, as shown in Fig. 1, and was sunk down to the bottom of the sea around after two days. Air pocket was expected for the rescue of many passengers inside of the ship. Objective of this study is to figure out the air pocket existence in the flooding & sinking accident using Marin Accident Integrated Analysis System (MAIAS; highly advanced M&S system of Fluid-Structure Interaction analysis technology [1, 2] using LS-DYNA code [3]). Several things were carried for this investigation of air pocket existence, such as accurate ship posture track according to accident duration using several accident photos and movies, precise ship and cargo moving track and sea water inflow amount according to accident duration using floating simulation and hydrostatic characteristics program, accurate understanding of exterior openings and interior paths of sea water inflow, simulation of sea water inflow using flooding & sinking simulation and calculation of exterior openings & interior inflow paths.

(a) April 06 11:18

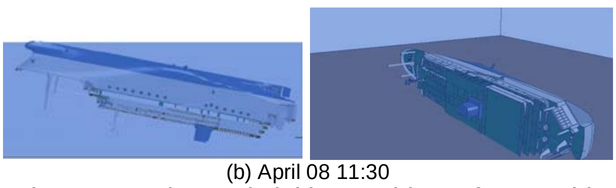

(b) April 08 11:30

Fig.1: Capsize and sinking accident of Ferry ship

3 Seawater Inflow Amount Estimation

For the exact estimation of seawater inflow amount into the inboard of ship, the followings were checked and carried out: flooding section modeling & volume according to deck, seawater inflow openings & inboard flooding paths, ship posture (fore & aft drafts, rolling angle) according to time, cargo shifting simulation according to ship posture, flooding situation reconstruction through survivor statements, inboard seawater inflow estimation according to elapsed time, and flooding & sinking simulation.

3.1 Flooding section modeling & volume according to deck

Figure 2 shows the Ro-Ro ferry ship and flooding section modeling, including chimney, for the estimation of seawater inflow amounts, where the maximum flooding and possible inflow amounts in decks are summarized in Table 1. Seawater inflow amounts of decks were supposed to be 99.5% of the maximum flooding amounts due to the diverse furniture, cargos, and engine, etc. Every deck Figure 3 illustrates the inboard whole tank flooding section modeling and void tank one, with their volume. The total volume of whole tanks and void tanks are 3,473.4 and 2,150.2 m^3, respectively.

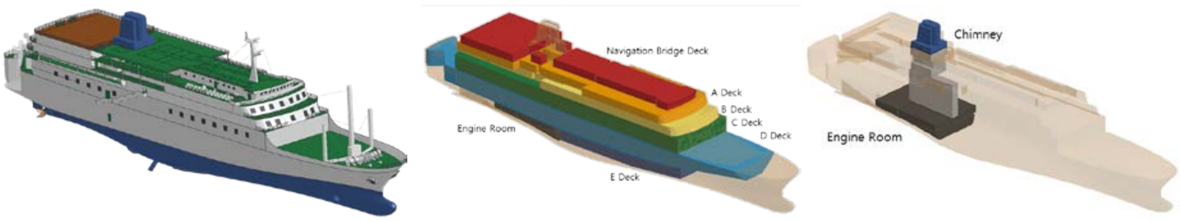

(a) Ro-Ro ferry ship modeling (b) flooding section modeling (c) engine room & chimney modeling

Fig.2: Ro-Ro ferry ship and flooding section modelings volume

Table 1: Amount of flooding section according deck

deck	maximum flooding amount (ton)	possible Inflow amount (ton)
Navigation bridge	2,651.70	2,638.44
A	4,218.20	4,197.11
B	4,304.90	4,283.38
C	9,851.30	9,802.04
D	14,470.40	14,398.05
E	3,914.10	3,894.53
Engine room	2,149.80	2,139.05
Total amount	41,560.40	41,352.60

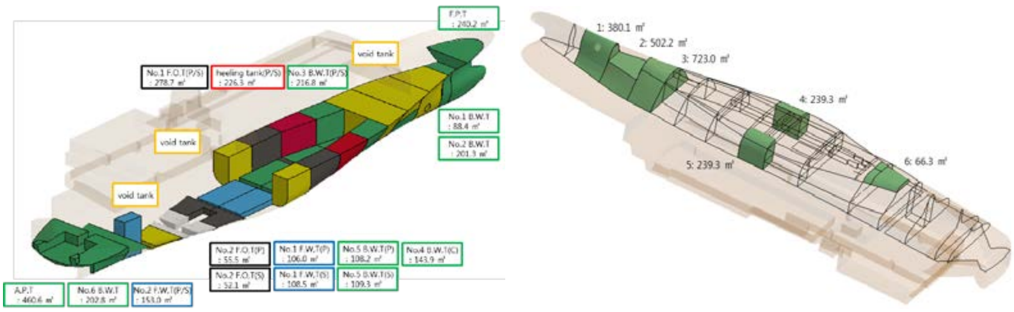

(a) total tanks (b) void tanks

Fig.3: Inboard tank modeling and its volume

3.2 Seawater inflow openings & inboard flooding paths

Seawater inflow openings and inboard flooding paths are very important for the estimation process of seawater flooding into the ship. Figure 4 shows their openings and flooding paths according to deck.

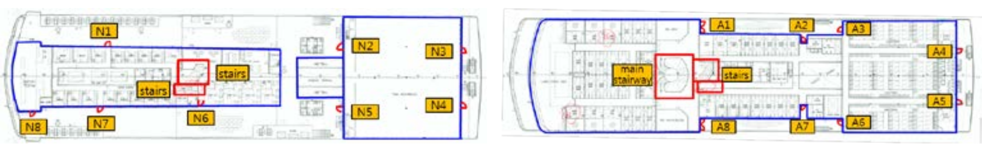

(a) Navigation bridge deck (b) A deck

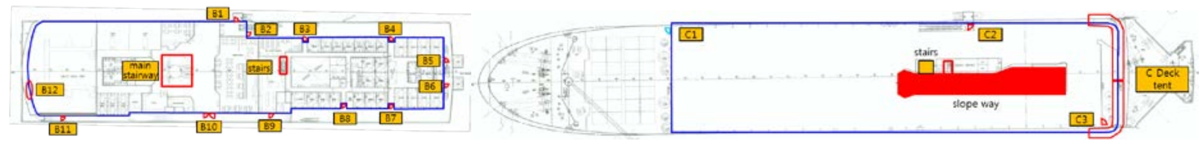

(c) B deck (d) C deck

(e) tent openings in C deck & Tween deck stern (1.4m & 1.2m height)

(f) D deck (g) D deck ramp (7.5m width & 4.2m height)

(h) D deck fright elevator (7.5m length & 3.5m height) & door (i) E deck

Fig.4: Seawater inflow openings & inboard flooding paths according to deck

The huge seawater inflow openings are the tent ones from the starboard to port sides at the stern in C deck & Tween deck, and the large indoor flooding paths are the stairway between A and B decks, and slope way between C and D decks.

3.3 Ro-Ro ferry ship posture (fore & aft drafts, rolling angle) according to time

Ro-Ro ferry ship postrure according to time, such as fore & aft drafts and rolling angle, was investigated based on the survey data of Joint Investigation Headquaters and 123 Coast Guard vessel. Figures 5 & 6 show the ship postures and their floating simulation reults according to time and their rolling angle and ceter of gravity responses, respectively. Table 2 summarizes their rolling angles and elapsed time from 8:50.

(a) 09:34:03, 52.2° heeling state (b) 09:39:10, 54.9° heeling state

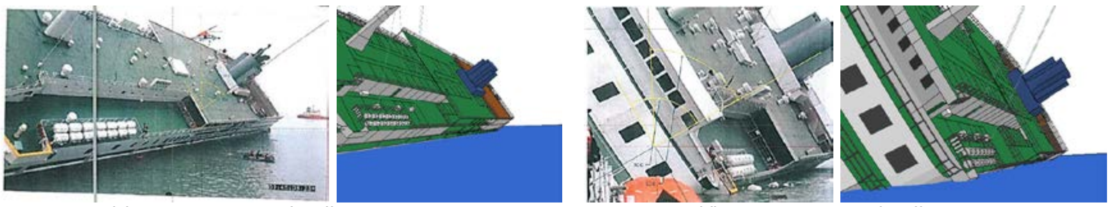

(c) 09:45:03, 57.3° heeling state (d) 09:50:22, 62.6° heeling state

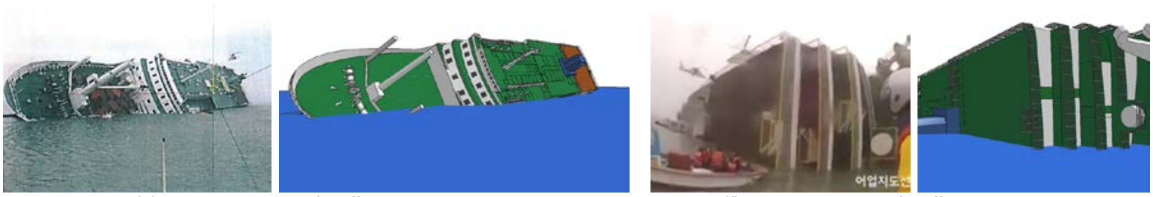

(e) 09:54:35, 64.4° heeling state (f) 10:15:36, 90.0° heeling state

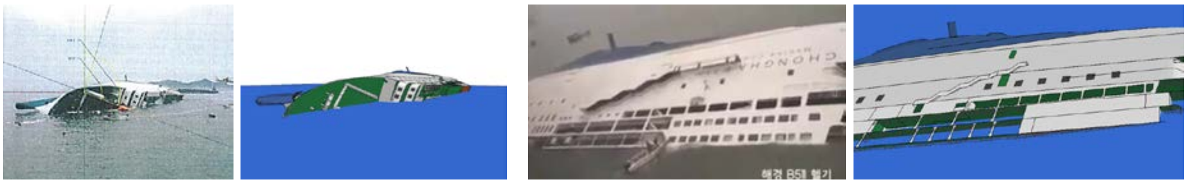

(g) 10:17:06, 108.1° heeling state (h) 10:18:15, 113.0° heeling state

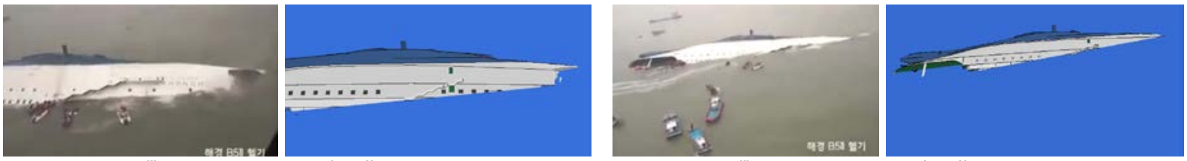

(i) 10:19:47, 115.4° heeling state (j) 10:20:36, 117.8° heeling state

(k) 10:21:15, 119.6° heeling state (l) 11:18:00, 180.0° heeling state

Fig.5: Ro-Ro ship posture according to time

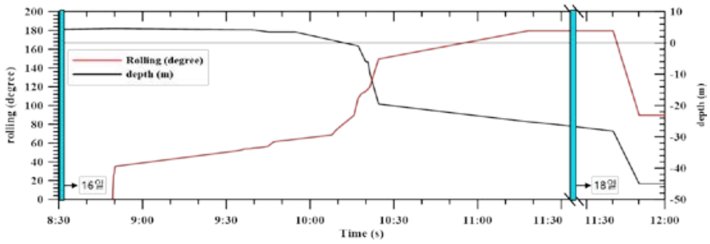

Fig.6: Rolling angle and ceter of ship response according to time

Table 2: Investigation based on survey data of Joint Investigation Headquarters & video of 123 Coast Guard vessel

	time	rolling angle (°)	elapsed time from 8:50 (sec)		time	rolling angle (°)	elapsed time from 8:50 (sec)
1	09:34:03	52.2	2,643	16	09:49:44	62.8	3,584
2	09:34:35	52.5	2,675	17	09:50:22	62.6	3,622
3	09:35:02	52.9	2,703	18	09:51:46	63.3	3,706
4	09:35:30	53.1	2,730	19	09:54:35	64.4	3,875
5	09:36:17	54.1	2,777	20	10:07:41	68.9	4,661
6	09:38:44	54.4	2,924	21	10:09:03	73.8	4,743
7	09:39:10	54.9	2,950	22	10:10:43	77.9	4,843
8	09:40:53	55.3	3,053	23	10:15:36	90.0	5,136
9	09:41:26	55.4	3,086	24	10:17:06	108.1	5,226
10	09:43:27	56.2	3,207	25	10:18:15	113.0	5,295
11	09:44:38	56.7	3,278	26	10:19:47	115.4	5,387
12	09:45:03	57.3	3,303	27	10:20:36	117.8	5,436
13	09:45:46	59.1	3,346	28	10:21:15	119.6	5,475
14	09:46:38	61.2	3,398	29	11:18:00	180.0	8,880
15	09:47:37	62.0	3,457				

3.4 Cargo shifting simulation and inboard seawater inflow according to ship posture

Cargo shifting simulation was carried out for the prediction of cargo shifting behaviors in the C forecastle & inboard decks, the estimation of inflow starting time of openings and the calculation of displacement according to the ship posture. Figure 7 shows the cargo shifting and ship capsize and sinking behaviors according to time. Seawater inflow starting and closing time of every opening was checked through the cargo shifting simulation and summarized by every step, as shown in Table 3.

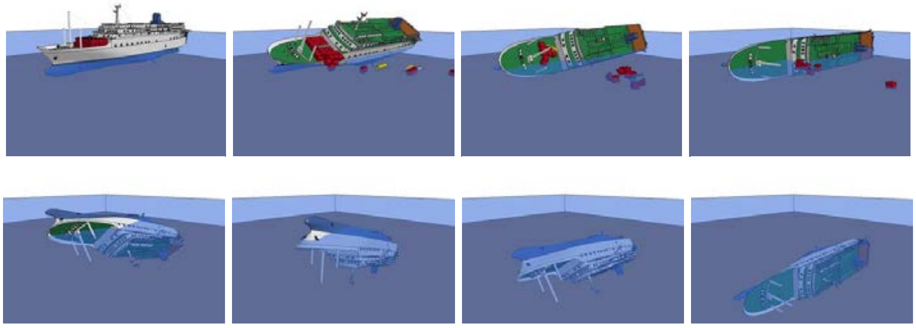

(a) stem port view

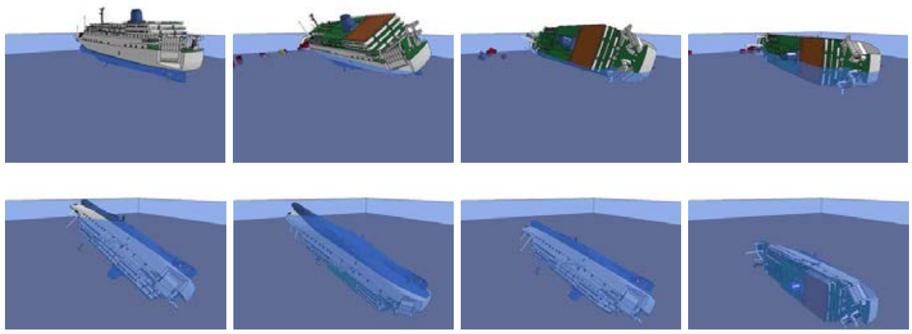

(b) stern port view

Fig.7: Cargo shifting simulation response vehavior according to ship posture

Table 3: Seawater inflow starting time through openings and rolling angle according to step

`		time	rolling angle (°)	seawater inflow starting & closure
1	1-1	08:49:18	13.8	Inflow through pilot door in D Deck, constant inflow & closure from 08:49:32 to 08:49:54
	1-2	08:49:43	27.3	Inflow through ramp in D Deck, constant inflow from 10:08:00
2	1 & 2	09:12:01	48.5	Inflow through stern door C3 in C Deck, constant inflow from 09:43:55
	2	09:22:10	49.2	Inflow through tent opening in C Deck, constant inflow from 10:18:53
3	2 & 3	09:48:25	62.3	Inflow through doors B9, B10 & A8 in B & A Decks, constant inflow from 09:54:52
	3 & 4	09:53:25	63.9	
4	4	09:54:52	64.5	Inflow through door A6 in A Deck, constant inflow from 10:00:24
	4 &5	09:59:06	65.6	
5	5	10:01:15	66.8	Inflow through doors B7 & B8 in B Deck, constant inflow from 10:04:10
	5 & 6	10:03:16	67.2	
6	6	10:07:41	68.9	Inflow through door N8 in Navigation Bridge Deck, constant inflow from 10:08:13
	6 & 7	10:08:00	70.0	
7	7-1	10:08:09	70.6	Inflow through door A7 in A Deck, constant inflow from 10:08:31
	7-2	10:08:19	71.2	Inflow through door A5 in A Deck, constant inflow from 10:09:44
	7-3	10:08:31	71.9	Inflow through doors N5 & N7 in Navigation Bri. Deck, constant inflow from 10:08:50 & 10:10:41
	7-5	10:08:41	72.5	Inflow through door N6 in Navigation Bri. Deck, constant inflow from 10:10:41
	7-6	10:09:51	74.9	Inflow through door B6 in B Deck, constant inflow from 10:10:41
	7 & 8	10:10:41	77.8	
8	8	10:11:20	79.1	Inflow through door B12 in B Deck, constant inflow from 10:12:25
9	8 & 9	10:13:16	84.2	
	9 & 10	10:15:36	90.0	
10	10-1	10:16:15	102.2	Inflow through door N3 in Navigation Bri. Deck, constant inflow from 10:16:32
	10-2	10:16:26	105.8	Inflow through door A4 in A Deck, constant inflow from 10:17:18
	10-3	10:16:27	106.0	Inflow through door N2 in Navigation Bri. Deck, constant inflow from 10:16:54
	10-4	10:16:32	107.0	Inflow through door N1 in Navigation Bri. Deck, constant inflow from 10:17:18
	10 & 11	10:17:18	109.0	
11	11-1	10:17:57	110.4	Inflow through doors B3, B4 & A2 in B & A Decks, constant inflow from 10:18:25
	11-2	10:18:39	111.5	Inflow through doors A3 & A1 in A Deck, constant inflow from 10:19:10 & 10:19:28
12	11 & 12	10:18:53	113.3	
	12 & 13	10:21:24	120.0	
13	13	10:23:31	140.1	Inflow through door C1 in C Deck, constant inflow from 10:23:41
14	13 & 14	10:24:33	150.0	
	14	11:18:00	180.0	

Volume under the ship surface could be estimated using cargo shifting simulation and hydrostatic characteristic program calculation at every rolling angle in each step. Maximum inboard inflow seawater amount was calculated by the difference of the ship displacement except falling cargos down to the seawater in C forecastle deck from the total displacement under the ship surface at typical rolling angle. Typical steps are introduced in the followings.

3.4.1 Step 3 (09:48:25~09:53:25, rolling angle 62.3°~63.9°)

Seawater inflow started inside the ship through the doors B9, B10 & A8 in B & A decks at rolling angle 62.3° on time 09:48:25, as shown in Fig. 8. The maximum inboard seawater inflow amount, 2,449.7 ton, was calculated, as shown in Table 4.

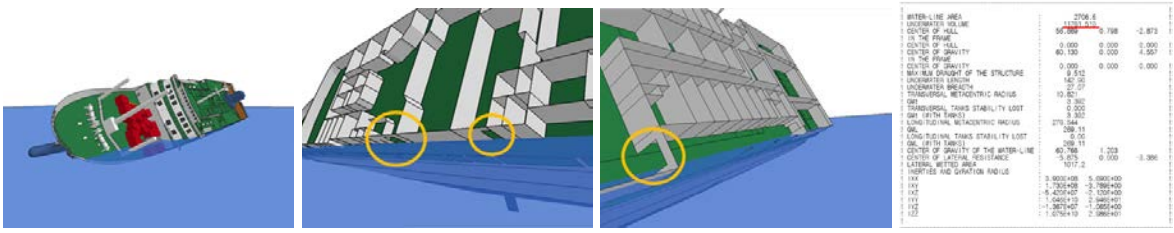

(a) stem port view (b) B9 & B10 doors in B deck (c) A8 in A deck (d) hydrostatics characteristic calculation

Fig.8: Floating simulation & hydrostatic characteristic calcultion of seawater inflow estimation in step 3

Table 4: Maximum inboard seawater inflow amount at rolling angle 62.3°

rolling angle 62.3°	volume under surface	displacement except falling cargos down to seawater in C forecastle deck	maximum inboard seawater inflow amount
0416 09:48:25	11,761.5 m^3	9,605.9 ton	2,449.7 ton

3.4.2 Step 10 (10:15:36~10:17:18, rolling angle 90.0°~109.0°)

Seawater inflow started inside the ship through the door N3 in Navigation Bridge deck at rolling angle 102.2° on time 10:16:15, and inboard seawater inflow are shown in Fig. 9. The maximum inboard seawater inflow amount, 18,950.0 ton, was calculated, as shown in Table 5. Every door in cabin decks, Navigation Bridge, A & B decks, has door ventilation and general office door handle, as shown in Fig. 10. Air Pocket could not be expected in the case of inboard seawater inflow in these cabin decks from this door condition.

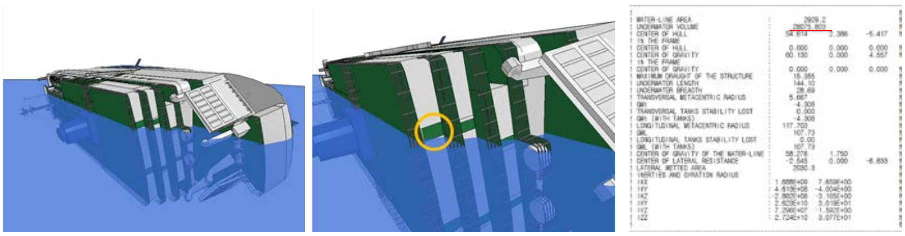

(a) stern port view (b) N3 door in Navi. Bri.deck (c) hydrostatics characteristic calculation

Fig.9: Floating simulation & hydrostatic characteristic calcultion of seawater inflow estimation in step 10

Table 5: Maximum inboard seawater inflow amount at rolling angle 102.2°

rolling angle 102.2°	volume under surface	displacement except falling cargos down to seawater in C forecastle deck	maximum inboard seawater inflow amount
0416 10:16:15	28,075.8 m^3	9,353.9 ton	18,950.0 ton

Fig.10: Door ventilation and generla office door handle at door in cabin decks

3.4.3 Step 14 (10:24:33~11:18:00, rolling angle 150.0°~180.0°)

Ship became capsized with most sections flooding, and stern cabins were touched to the bottom of the sea at rolling angle 180.0° on time 11:18:00, as shown in Fig. 11. The maximum inboard seawater inflow amount, 40,936.1 ton, was calculated, as shown in Table 6.

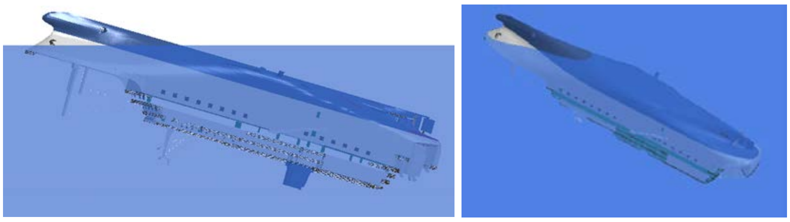

(a) capsize

(b) hydrostatics characteristic calculation

Fig.11: Floating simulation & hydrostatic characteristic calcultion of seawater inflow estimation in step 14

Table 6: Maximum inboard seawater inflow amount at rolling angle 180.0°

rolling angle 180.0°	volume under surface	displacement except falling cargos down to seawater in C forecastle deck	maximum inboard seawater inflow amount
0416 11:18:00	49,063.4 m^3	9,353.9 ton	40,936.1 ton

3.5 Rapid turning capsize & flooding situation reconstruction through survivor statements

Rapid turning capsize and inboard flooding situations could be reconstructed through the statements of several survivors, and their statements were very helpful to figure out the real whole and detailed situations even though they could not remember the exact time and rolling angle. Figure 8 typically illustrates their two statements.

(a) Mr. Ko

(b) Mrs. Lee

(c) escape paths of Mr. Ko & Mrs. Lee in B deck

Fig.12: Rapid turning capsize & flooding situation, escape paths in survivor statements

3.6 Accumulated inboard seawater inflow estimation

Accumulated inboard seawater inflow amount was calculated through the openings according the ship posture, as shown in Table 3, estimating the flooding gap or area of each opening and its inflow interval duration, and checking the subtotal accumulated inboard seawater inflow amount calculation with the maximum inboard seawater inflow amount using floating simulation and hydrostatic characteristic calculation, as shown in Tables 4-6. Since their calculation procedures were very huge one, here their subtotal amounts are summarized in Table 7. Table 8 summarizes the inboard seawater inflow amount into each deck through exterior openings & the ratio to its maximum deck seawater inflow amount, and Fig. 13(a) shows their inflow amount responses according to time (step). It could be found that 62.9% of seawater inflow total amount was flowed into C deck through its openings, and especially 52.3%, through the stern tent opening of C deck, as shown in Tables 7 & 8. Seawater inflow started at the rolling angle 49.2° through the tent opening, and rapidly increased at the rolling angle 68.9° (10:07:41), as shown in Table 3 and Fig. 13, with capsize within around 2.5 hours. Table 9 shows the seawater transference through the inboard paths, and most of decks were flooded at 11:18:00, except engine room and D deck.

Table 7: Accumulated seawater inflow amount through openings

deck	Inflow opening (step)	subtotal flooding amount (ton)	total amount (ton)	deck	Inflow opening (step)	subtotal flooding amount (ton)	total amount (ton)
D	pilot door (1-1)	343.55		A	A7 (7-1)	1,134.79	
	ramp (1-2)	2,437.50	2,781.05		A5 (7-2)	743.85	
C	C3 (1 & 2)	4,266.65(10.5%)			A4 (10-1)	104.67	
	stern tent (2)	21,317.81(52.3%)			A2 (11-1)	95.46	
	C1 (12)	63.77(0.2%)	25,648.23		A3 (11-2)	58.78	
B	B12 (2 & 3)	1,941.37			A1 (11-2)	55.55	4,732.35
	B9 (2 & 3)	885.00		Navi. Bridge	N8 (6)	564.84	
	B8 (5)	529.11			N5 (7-3)	698.85	
	B7 (5)	529.11			N7 (7-3)	521.77	
	B6 (7-5)	449.55			N6 (7-4)	397.82	
	B12 (8)	294.96			N3 (8 & 9)	243.09	
	B3 (11-1)	126.82			N2 (10-2)	191.77	
	B4 (11-1)	83.18	4,839.10		N1 (10-3)	167.64	2,785.79
A	A8 (2 & 3)	1,694.51		sum total flooding amount			40,786.52
	A6 (4)	844.74					

Table 8: Inboard seawater inflow amount & ratio into each deck according to step

step	time	rolling angle (°)	D Deck 14,398.05 ton (%)	C Deck 9,802.04 ton (%)	B Deck 4,283.38 ton (%)	A Deck 4,197.11 ton (%)	Nav. Bri. Deck 2,638.44 ton (%)	total amount (ton)
1	9:12:01	48.5	551.61	-	-	-	-	551.61
2	9:48:25	62.3	1,508.04	941.64	-	-	-	2,449.68
3	9:53:25	63.9	1,686.12	1,748.77	9.23	19.72	-	3,463.84
4	9:59:06	65.6	1,911.50	3,532.74	45.23	67.95	-	5,557.42
5	10:03:17	67.2	2,107.06	5,962.49	330.25	111.39	-	8,511.19
6	10:08:00	70.0	2,407.42	8,865.04	598.25	473.40	1.91	12,346.02
7	10:10:41	77.8	2,579.70	9,127.67	1,325.05	1,111.63	264.17	14,408.22
8	10:13:16	84.2	2,662.64	9,489.91	1,951.38	1778.90	677.25	16,560.08
9	10:15:36	90.0	2,737.54	9,812.78	2,545.88	2,377.81	1,137.24	18,611.25
10	10:17:18	109.0	2,753.92	10,868.74	3,146.12	2,887.44	1,676.74	21,332.96
11	10:18:53	113.3	2,764.21	15,746.84	3,789.18	3,451.66	2,267.15	28,019.04
12	10:21:24	120.0	2,777.67	23,439.15	4,615.68	4,258.39	2,580.72	37,671.61
13	10:24:33	150.0	2,778.18	23,955.33	4,666.53	4,554.85	2,621.40	38,576.29
14	11:18:00	180.0	2,781.05(19.3)	25,648.23(261.7) (62.9% total)	4,839.10(113.0)	4,732.35(112.8)	2,785.79(105.6)	40,786.52

Table 9: Accumulated seawater inflow amount into each deck after transfeence through inboard paths

step	time	Engine room 2,139.05 ton	E Deck 3,894.53 ton	D Deck 14,398.05 ton	C Deck 9,802.04 ton	B Deck 4,283.38 ton	A Deck 4,197.11 ton	Navi. Bri. Deck 2,638.44 ton	total amount (ton)
1	9:12:01	-	-	551.61	-	-	-	-	551.61
2	9:48:25	-	-	1,508.04	941.64	-	-	-	2,449.68
3	9:53:25	-	-	1,686.12	1,748.77	9.23	19.72	-	3,463.84
4	9:59:06	-	240.68	1,670.82	3,532.74	45.23	67.95	-	5,557.42
5	10:03:17	-	417.84	4,092.96	3,558.75	330.25	111.39	-	8,511.19
6	10:08:00	544.76	617.59	6,297.94	3,812.17	598.25	473.40	1.91	12,346.02
7	10:10:41	854.68	731.22	6,147.53	3,973.94	1,325.05	1,111.63	264.17	14,408.22
8	10:13:16	1,153.05	840.63	5,944.00	4,214.87	1,951.38	1,778.90	677.25	16,560.08
9	10:15:36	1,422.54	939.44	5,757.27	4,431.07	2,545.88	2,377.81	1,137.24	18,611.25
10	10:17:18	1,618.88	1,011.43	5,677.99	5,314.36	3,146.12	2,887.44	1,676.74	21,332.96
11	10:18:53	1,801.75	1,078.49	8,452.71	7,178.10	3,789.18	3,451.66	2,267.15	28,019.04
12	10:21:24	2,092.42	1,185.06	13,973.30	9,359.62	4,283.38	4,197.11	2,580.72	37,671.61
13	10:24:33	2,139.05	1,318.46	14,264.10	9,752.79	4,283.38	4,197.11	2,621.40	38,576.29
14	11:18:00	2,139.05	3,582.01	14,144.49	9,802.04	4,283.38	4,197.11	2,638.44	40,786.52

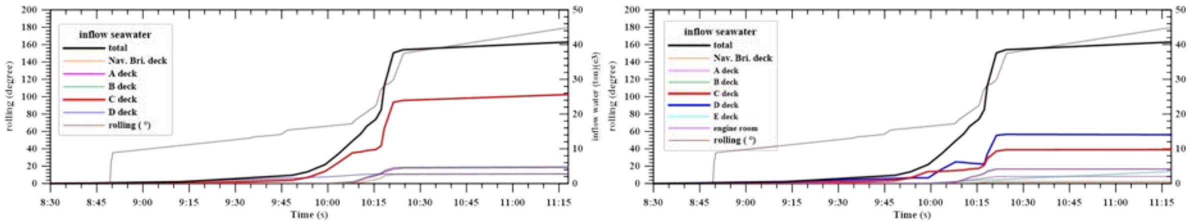

(a) inboard seawater inflow amount from openings (b) accumulated seawater inflow amount through paths

Fig.13: Inboard an accumulated seawater inflow amount response according to deck through exterior openings and internal paths

4 Flooding & Sinking Simulation

Three cases of flooding & sinking simulations were carried out during 13.8°~48.5°, 70.0°~90.0°, and 109.0°~150.0°, respectively. Through the flooding & sinking simulations, the estimation of accumulated seawater inflow amount of each deck through the exterior openings and interior paths, as shown in Tables 7~9, was verified, seawater inflow and transferring behaviors through the openings and paths were confirmed, and shifting behaviors of cargos and vehicles in flooded decks with were also compared with those of them in void ones.

4.1 Case 1: rolling angle 13.8°~48.5° during 8:49:18~9:12:01

Seawater inflow started into the pilot door in D deck at rolling angle 13.8°, and through the port side ramp at rolling angle 27.3°, during rapid turning. Flooding & sinking simulation was conducted until rolling angle 48.5°. As shown in Fig. 14, seawater was flowed into the pilot door until showdown at rolling angle 35.0°due to the shift of vehicle to the door, and through the gap of ramp and stern part. Around 551.6 ton of seawater was flooded at the stern port side of D deck during around 22.5 minutes.

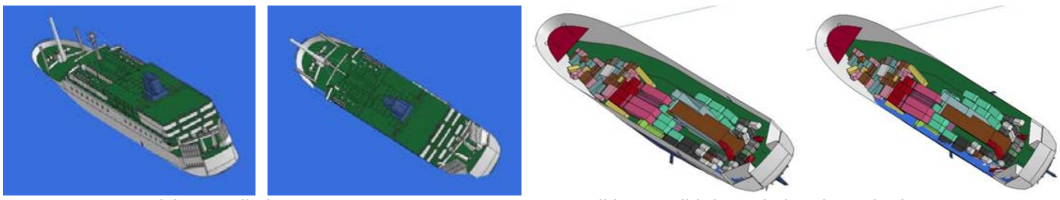

(a) overall view (b) overall inboard view in C deck

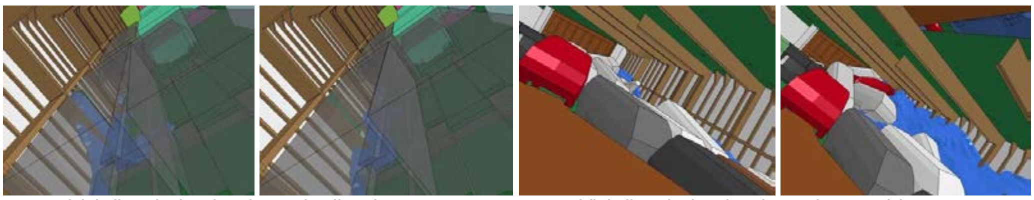

(c) inflow behavior through pilot door (d) inflow behavior through port side ramp

Fig.14: Seawater inflow behavior in Case 1: rolling angle 13.8°~48.5° during 8:49:18~9:12:01

4.2 Case 2: rolling angle 70.0°~90.0° during 10:08:00~10:15:36

Rapid upright heeling state occurred with a lot of seawater inflow through tent opening in C Deck stern, and a lot of seawater also flowed into the A, B and Navigation Bridge decks through the port side door openings. Figure 15 shows the seawater inflow and transferring behaviors through the openings and paths, and shifting behaviors of cargos and vehicles in each deck in Case 2. It could be confirmed that total seawater inflow amount was around 6,265.2 ton, around 328.8 ton, 321.9 ton and 877.8 ton were transferred from C deck to D deck, from D deck to Engine room and E deck, respectively, during 456.0 seconds, and there was around 1,422.5 ton, 939.4 ton, 5,757.3 ton, 4,431.1 ton, 2,545.9 ton, 2,377.8 ton, and 1,137.2 ton in Engine room, E, D, C, B, A and Navigation Bridge decks, respectively.

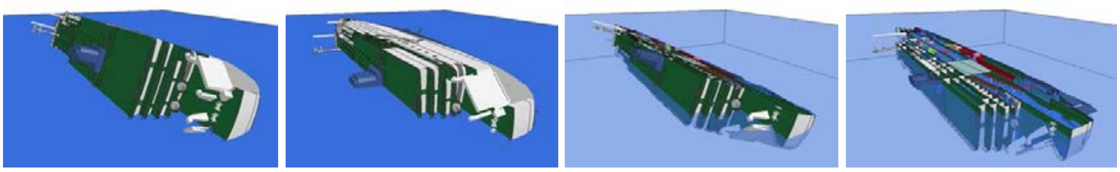

(a) overall view (b) overall view with logitidinal section

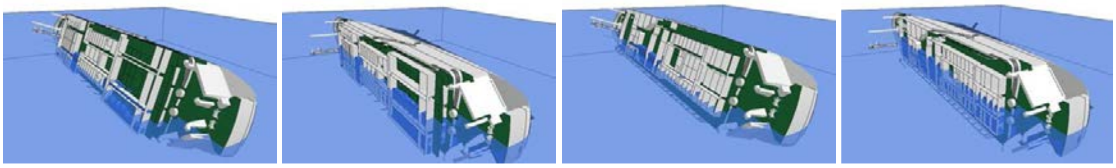

(c) A deck (d) B deck

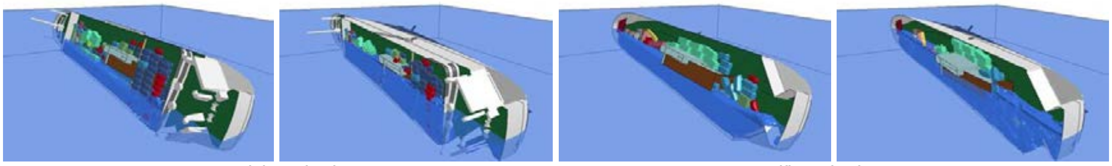

(e) C deck (f) D deck

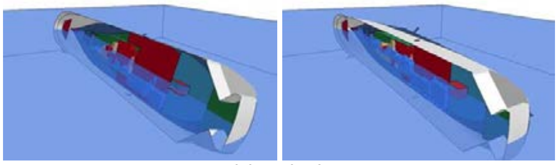

(g) E deck

Fig.15: Seawater inflow behavior in Case 2: rolling angle 70.0°~90.0° during 10:08:00~10:15:36

4.3 Case 3: rolling angle 109.0°~150.0° during 10:17:18~10:24:33

Most cabins were sunk under surface from the stern part due to seawater flooding in C & D decks, and bulbous bow & bottom tank parts were also floating above surface due to big heeling. Figure 16 illustrates the seawater inflow and transferring behaviors through the openings and paths, and shifting behaviors of cargos and vehicles in each deck in Case 3. It could be confirmed that total seawater inflow amount was around 17,243.0 ton, around 12,999.0 ton was through the tent opening in C deck, during 435.0 seconds, and that around 8,648.0 ton was transferred from the C deck to D deck through the slope way and around 307.0 ton and 520.0 ton, from D deck to E deck and Engine room, respectively.

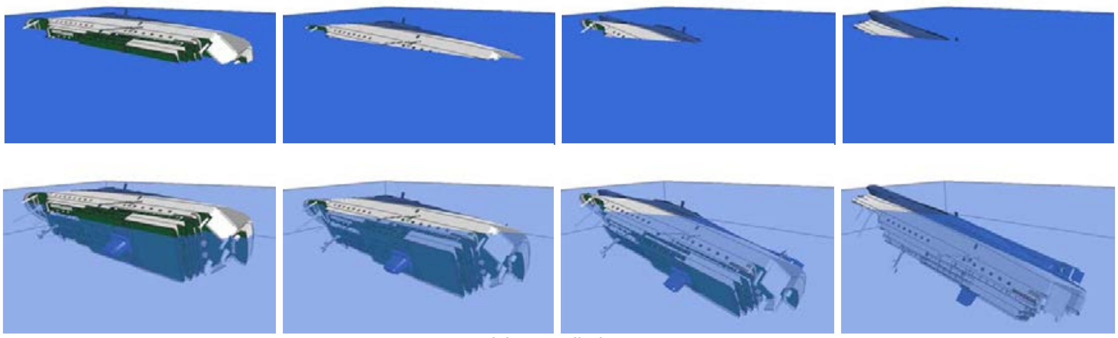

(a) overall view

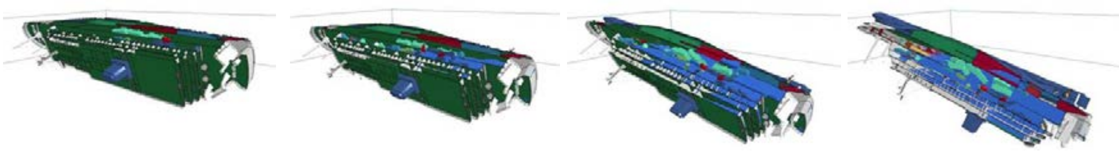

(b) overall view with logitidinal section

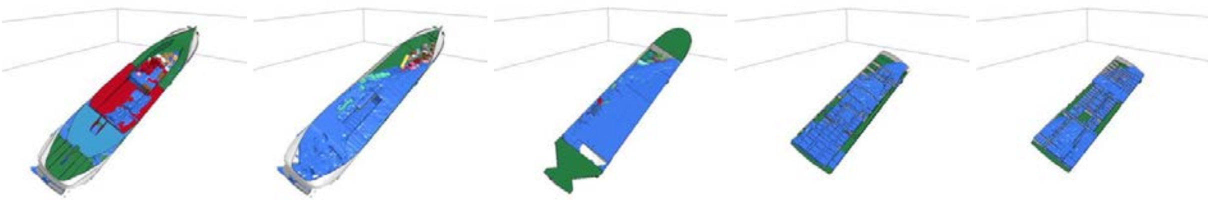

(c) E deck (d) D deck (e) C deck (f) B deck (g) A deck

Fig.16: Seawater inflow behavior in Case 3: rolling angle 109.0°~150.0° during 10:17:18~10:24:33

5 Investigation of Air Pocket

The statement of a man survivor in the cabin under the very rapid seawater inflow state was such that seawater inflow touched his foot to head within just 9.0 seconds. As mentioned from Fig. 10, Air pocket could not be expected in the case of inboard seawater inflow in the cabin decks, since every door had a ventilation and general office door handle. Flooding amount and air region was analyzed using floating simulation and hydrostatic characteristic calculation from the capsizing to sinking stages, as shown in Fig. 17 and Table 10. Table 11 summarizes the inboard seawater inflow amount in each deck according to time. Whereas there was an air pocket region in D & E decks at the first capsizing situation at 11:18:00 on April 16, there was no air pocket region in every deck and, moreover, inboard seawater inflow amount exceeded the total possible inboard flooding amount at the second and third capsizing situations. Escape pipe is connected at the tank to the main deck, and seawater inflow is usually protected from the main deck. However, the protector might be destroyed because of long period usage. Table 12 summarizes the seawater inflow amounts into the several tanks through the escape pipes. Ferry ship was sunk a little bit more at 13:00:00 on April 16 after 102 minutes due to the seawater inflow amount 1,754.62 ton through the escape pipes, and was sunk down at last under the surface at 11:40:00 on April 18 after 46 hours and 40 minutes with seawater inflow amount 573.80 ton through escape pipes.

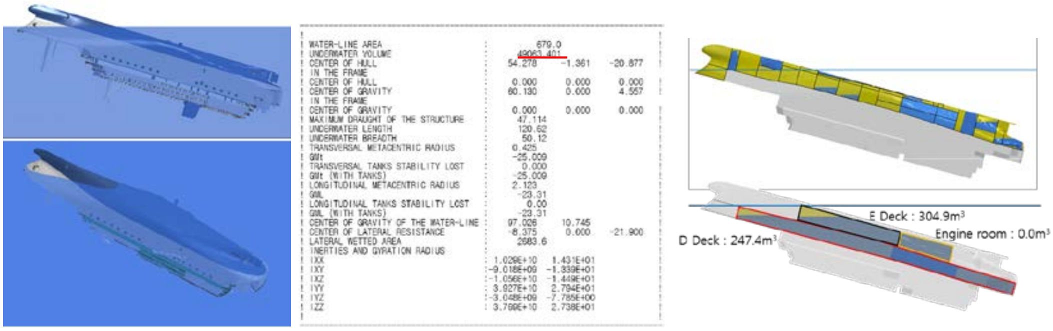

(a) rolling angle 180.0° at 11:18:00 on April 16

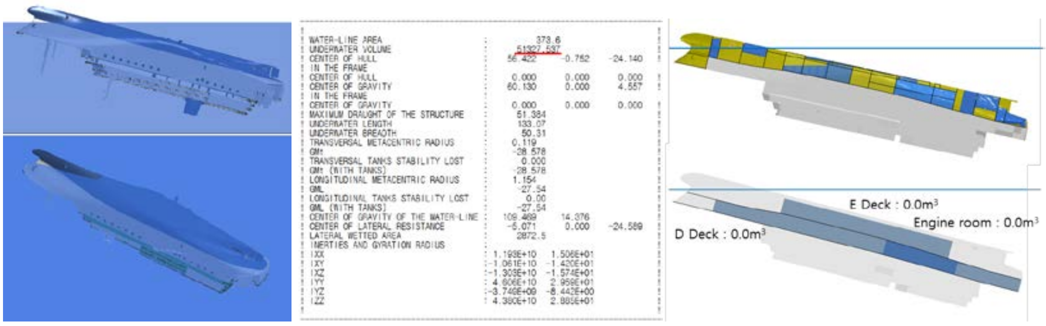

(b) rolling angle 180.0° at 13:00:00 on April 16

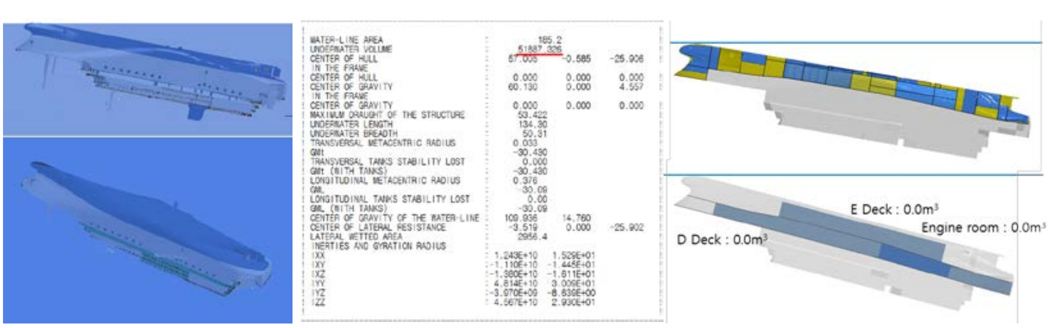

(c) rolling angle 180.0° at 11:40:00 on April 18

Fig.17: Floating simulation and hydrostatic characteristic calculation of capsizing situation

Table 10: Inboard seawater inflow amount of capsizing situation accoding to time

time	volume under surface (m^3)	displacement except dropped cargos (ton)	inboard seawater inflow amount (ton)
0416 11:18:00	49,063.4	9,353.9	40,936.1
0416 13:00:00	51,327.5	9,353.9	43,256.8
0418 11:40:00	51,887.3	9,353.9	43,830.6

Table 11: Inboard seawater inflow amount of capsizing situation in each deck according to time

Deck	possible inboard flooding amount (ton)	11:18:00 on Apr.16	13:00:00 on Apr.16	11:40:00 on Apr.18
Navi. bridge	2,638.44	2,638.44 (100%)	2,638.44 (100%)	2,638.44 (100%)
A	4,197.11	4,197.11 (100%)	4,197.11 (100%)	4,197.11 (100%)
B	4,283.38	4,283.38 (100%)	4,283.38 (100%)	4,283.38 (100%)
C	9,802.04	9,802.04 (100%)	9,802.04 (100%)	9,802.04 (100%)
D	14,398.05	14,144.49 (98%)	14,398.05 (100%)	14,398.05 (100%)
E	3,894.53	3,582.01 (92%)	3,894.53 (100%)	3,894.53 (100%)
Engine	2,139.05	2,139.05 (100%)	2,139.05 (100%)	2,139.05 (100%)
Total	41,352.60	40,786.52	41,352.60	41,352.60
		40,936.10	43,256.80	43,830.60

Table 12: Inboard seawater inflow amount of capsizing situation in each deck according to time

Tank		*at accident*	11:18:00 on Apr.16	13:00:00 on Apr.16	11:40:00 on Apr.18
Ballast Water Tank	F.P.T	0.00	5.87(**+5.87**)	102.56(**+96.69**)	246.16(**+143.60**)
	No.1 B.W.T	82.00	82.00	90.61(**+8.61**)	90.61
	No.2 B.W.T	200.12	200.12	206.37(**+6.25**)	206.37
	No.3 B.W.T(P&S)	0.00	13.35(**+13.35**)	300.59(**+287.24)**	444.44(**+143.85**)
	No.4 B.W.T	143.08	143.08	147.49(**+4.41**)	147.49
	No.5 B.W.T(P&S)	216.17	216.17	222.94(**+6.77**)	222.94
	No.6 B.W.T	0.00	19.03(**+19.03**)	207.87(**+188.84**)	207.87
	A.P.T	0.00	17.30(**+17.30**)	302.17(**+284.87**)	472.12(**+169.95**)
	heeling tank(P&S)	102.60	116.63(**+14.03**)	347.50(**+230.87**)	463.90(**+116.40**)
Inflow amount through escape pipe		-	**69.58**	**1,114.55**	**573.80**
Ballast Water Tank		743.97	813.55	1,928.10	2,501.900
Fresh Water Tank	No.1 F.W.T(P&S)	45.00	61.52(**+16.52**)	218.74(**+157.22**)	218.74
	No.2 F.W.T (C)	147.00	147.00	153.15(**+6.15**)	153.15
Fuel Oil Tank	No.1 F.O.T(P)	49.400	64.08(**+14.68**)	281.77 (**+217.69**)	281.77
	No.1 F.O.T(S)	49.400	64.08(**+18.42**)	281.77 (**+217.69**)	281.77
	No.2 F.O.T(P)	14.800	31.86(**+17.06**)	54.26(**+22.40**)	54.26
	No.2 F.O.T(S)	14.800	31.86(**+17.06**)	50.78(**+18.92**)	50.78
Inflow amount through escape pipe		**-**	**80.00**	**640.07**	**0.0**
F.W.T Tank & Fuel Oil Tank Total		320.40	400.40	1,040.47	1040.47
Total inflow amount through escape pipe		0.00	**149.58**	**1,754.62**	**573.80**
Tank Total		1,064.37	1,213.95	2,968.57	3,542.37

6 Considerations

Inboard seawater flooding process was realized through the floating simulation and hydrostatic characteristic program calculation, and full-scale ship flooding & sinking simulation using MAIAS (highly advanced M&S system of Fluid-Structure Interaction analysis technique). It could be confirmed that inboard seawater flooding of Ro-Ro ferry ship might be relatively precisely estimated according to flooding, capsizing and sinking accident process, there was no air pocket in the cabin decks, the bow part could be floating for a while due to the air in the several tanks and void ones at the bottom, and the ferry ship was turned over very rapidly due to a lot of seawater inflow through huge openings covered by tents at the stern of C & Tween deck.

7 Acknowledgement

This research was performed by the support of Special Investigation Commission on 4/16 Sewol Ferry Disaster. The authors would like to express our appreciation to their supports.

8 Literature

[1] Aquelet, N., Souli, M., and Olovsson, L., Euler–Lagrange coupling with damping effects: Application to slamming problems, Computer Methods in Applied Mechanics and Engineering, 195, (2006), 110–132.

[2] Souli, M., Ouahsine, A., and Lewin, L., ALE formulation for fluid-structure interaction problems, Computer Methods in Applied Mechanics and Engineering, 190, (2000), 659-675.

[3] LSTC, LS-DYNA User's Manual, Version 971 R7, Livermore Soft Technology Corp., USA, (2013).